

## Research

# Targeting EFNA1 suppresses tumor progression via the cMYC-modulated cell cycle and autophagy in esophageal squamous cell carcinoma

Houxiang Jiang<sup>1,2</sup> · Shaoxiang Wang<sup>3</sup> · Ying Liu<sup>4</sup> · Chaopan Zheng<sup>5</sup> · Lipeng Chen<sup>4</sup> · Kai Zheng<sup>3</sup> · Zhenyu Xu<sup>6</sup> · Yong Dai<sup>4</sup> · Hongtao Jin<sup>7</sup> · Zhiqiang Cheng<sup>7</sup> · Chang Zou<sup>4,8</sup> · Li Fu<sup>9</sup> · Kaisheng Liu<sup>4</sup> · Xiaoshi Ma<sup>10</sup>

Received: 15 February 2023 / Accepted: 19 April 2023

Published online: 09 May 2023

© The Author(s) 2023 **OPEN**

## Abstract

**Purpose** Esophageal squamous cell carcinoma (ESCC) remains one of the most common causes of cancer death due to the lack of effective therapeutic options. New targets and the targeted drugs are required to be identified and developed.

**Methods** Highly expressed genes in ESCA were identified using the edgeR package from public datasets. Immunostaining assay verified the high expression level of EFNA1 in ESCC. CCK-8, colony formation and wound healing assays were performed to examine the role of EFNA1 and EPHA2 in ESCC progression. Cell cycle was analyzed by flow cytometry and autophagy activation was determined by autophagolysosome formation using transmission electron microscopy. The small molecule targeting to EFNA1 was identified by molecular docking and the anti-tumor effects were verified by in vitro and in vivo models with radiation treatment.

**Results** EFNA1 was highly expressed in esophageal cancer and significantly associated with poor prognosis. Down-regulation of EFNA1 remarkably inhibited cell proliferation and migration. Furthermore, decreased EFNA1 significantly suppressed the expression of cMYC along with its representative downstream genes involved in cell cycle, and activated autophagy. Similar effects on ESCC progression were obtained from knockdown of the corresponding receptor, EPHA2. The potential small molecule targeting to EFNA1, salvianolic acid A (SAA), could significantly suppress ESCC progression and increase the sensitivity to radiotherapy.

Houxiang Jiang, Shaoxiang Wang, Ying Liu and Chaopan Zheng contributed equally to this work

**Supplementary Information** The online version contains supplementary material available at <https://doi.org/10.1007/s12672-023-00664-9>.

✉ Li Fu, [gracelfu@szu.edu.cn](mailto:gracelfu@szu.edu.cn); ✉ Kaisheng Liu, [liukaisheng@szhospital.com](mailto:liukaisheng@szhospital.com); ✉ Xiaoshi Ma, [ma.xiaoshi@szhospital.com](mailto:ma.xiaoshi@szhospital.com) | <sup>1</sup>Department of Gastrointestinal Surgery, The First Affiliated Hospital of Wannan Medical College (Yijishan Hospital of Wannan Medical College), Wuhu 241001, Anhui, China. <sup>2</sup>Anhui Province Clinical Research Center for Critical Respiratory Medicine, Wuhu 241001, Anhui, China. <sup>3</sup>School of Pharmaceutical Sciences, Health Science Center, Shenzhen University, Shenzhen 518060, China. <sup>4</sup>Guangdong Provincial Clinical Research Center for Geriatrics, Shenzhen Clinical Research Center for Geriatrics, Shenzhen People's Hospital (The Second Clinical Medical College of Jinan University), Shenzhen 518020, Guangdong, China. <sup>5</sup>Department of Otolaryngology, Shenzhen People's Hospital (The Second Clinical Medical College of Jinan University), Shenzhen 518020, Guangdong, China. <sup>6</sup>Precision Medicine Center, The First Affiliated Hospital of Wannan Medical College (Yijishan Hospital of Wannan Medical College), Wuhu 241001, Anhui, China. <sup>7</sup>Department of Pathology, Shenzhen People's Hospital (The Second Clinical Medical College of Jinan University), Shenzhen 518020, Guangdong, China. <sup>8</sup>School of Medicine, Life and Health Sciences, The Chinese University of Hong Kong, Shenzhen 518172, Guangdong, China. <sup>9</sup>Department of Pharmacology, Shenzhen University School of Medicine, Shenzhen 518060, Guangdong, China. <sup>10</sup>Department of Urology, Shenzhen People's Hospital (The Second Clinical Medical College of Jinan University), Shenzhen 518020, Guangdong, China.



**Conclusion** We revealed that *EFNA1* facilitated the ESCC progression via the possible mechanism of activating cMYC-modulated cell proliferation and suppressing autophagy, and identified SAA as a potential drug targeting *EFNA1*, providing new options for the future treatments for ESCC patients.

**Keywords** *EFNA1* · Esophageal squamous cell carcinoma · cMYC · Autophagy · Salvianolic acid A

## 1 Introduction

Esophageal cancer (ESCA) is the 7th most frequently diagnosed malignant carcinoma and the 6th leading cause of cancer-related death worldwide [1]. It is mainly consisted of two histological subtypes, the esophageal adenocarcinoma and esophageal squamous cell carcinoma (ESCC). Approximately 90% of ESCA patients will be further diagnosed as ESCC, a more aggressive and lethal type with only 26.2% of 5-year postoperative survival rate [2]. Although patients could get benefits from the development of current treatments like surgical resection, radiotherapy and chemotherapy, the outcomes are still unsatisfactory [3]. Plus, the preoperative cisplatin and 5-fluorouracil-based chemotherapy or radiotherapy for down-stage the disease usually bring severe side effects for the patients, even would cause a delay in surgery for patients who respond poorly [4, 5].

With the advances in high-throughput sequencing technologies, critical molecules involved in ESCC progression have been unveiled gradually, including *EGFR*, *HER-2*, *VEGFR* as well as some epigenetic molecules [6–8]. The targeted drugs have soon been developed and proven effective to improve the prognosis of ESCC patients at different levels [9–11]. Despite of the progress we have achieved in recent years, unstable efficacies, drug resistance for patients with mutations in related genes or severe adverse effects have limited the applications of these target drugs [12]. New targets and the targeted drugs are required to be identified and developed to overcome these limitations.

*EFNA1* is a member of ephrin family which has been reported to be involved in multiple malignant progresses like tumor growth, invasiveness and metastasis [13–15]. In hepatocellular carcinoma, Lida et al. showed that increased expression of *EFNA1* could significantly promote tumor growth by the potential downregulation of cell cycle inhibitor p21 and upregulation of angiogenesis factor angiopoietin 1 [16]. In mesothelioma, *EFNA1* could suppress the tumor growth via the induction of miR-320b-regulated apoptosis and the miRNA let-7-mediated repression of the RAS expression [17, 18]. However, the exact role of *EFNA1* in ESCC progression and the potential value in ESCC treatment have barely been explored and remain unknown.

Here, we integrated different public datasets and identified *EFNA1* with the most significant correlations with ESCA progression and dismal prognosis. Knockdown of *EFNA1* significantly suppressed proliferation and migration of ESCC cells under the potential regulation of cMYC and autophagy signaling pathways. Salvianolic acid A (SAA), screened as a small molecular medicine targeting *EFNA1* via molecular docking, showed significant inhibitory effects on ESCC cell proliferation and tumor growth. The additional SAA treatment upon radiation remarkably increased the sensitivity of ESCC to radiation therapy, suggesting a novel therapeutic option for ESCC in future administrations.

## 2 Materials and methods

### 2.1 Expression analysis of ESCA patients

RNA-seq profiles and clinical data of 160 patients with ESCA were obtained from the TCGA database. Differentially expressed genes (DEGs) were identified using the edgeR package and filtered by fold change > 2, *p* value < 0.05 and false discovery rate < 0.05. They were further validated in four other gene expression omnibus datasets including GSE23400, GSE29001, GSE33426 and GSE38129. The overlapped genes were considered as potentially critical genes in ESCA progression.

## 2.2 Immunostaining

The human ESCC tissue microarray (HEsoS180Su07, Shanghai Outdo Biotech Co. Ltd., China), consisted of 63 cancerous tissues and the corresponding normal tissues, was used to examine the expression characteristic of *EFNA1*. Immunostaining assay was performed as described by Yu et al. (2013) using the anti-*EFNA1* antibodies (diluted at 1:200, Abcam, cat. no. ab238505) and the HRP-conjugated secondary antibody (diluted at 1:2000, Abcam, cat. no. ab7090). The *EFNA1* staining score was evaluated by two qualified pathologists based on the staining rate and intensity.

## 2.3 Construction of *EFNA1* knockdown cells with shRNA

Two shRNAs were used to suppress the expression of *EFNA1* in ESCC cell lines (Additional file 4: Table S1). The non-targeting scrambled shRNA-NC contained a sequence with no significant homology to any known human gene (HANBIO Co. Ltd., China). Virus packaging and cell transfection were performed as described previously [19].

## 2.4 qRT-PCR

Total RNA was extracted using the RNeasy Mini Kit (QIAGEN GmbH, cat. no. 74104, Germany) according to manufacturer's instructions. The cDNA synthesis was performed using a PrimeScript RT Master Mix kit (Takara, China) according to manufacturer's instruction. qRT-PCR was performed using the TB Green Premix EX Taq II system with a Roche LightCycler 96 qPCR instrument (Roche Diagnostics, Germany). The primer sequences used in this study were listed in Additional file 5: Table S2. Gene relative expression levels were normalized to *GAPDH* expression and analyzed using the  $2^{-\Delta\Delta Ct}$  method.

## 2.5 Western blot

The expression levels of candidate proteins were examined by western blot analysis as previously described [20]. The antibodies were anti- $\beta$ -actin (diluted at 1:1000, CST, cat. no. 3700S), anti-GAPDH (diluted at 1:1000, CST, cat. no. 5174S), anti-AKT (diluted at 1:1000, CST, cat. no. 4691S), anti-p-AKT (diluted at 1:1000, CST, cat. no. 4060S), anti-p-CDC2 (diluted at 1:1000, CST, cat. no. 4539S), anti-cMYC (diluted at 1:1000, CST, cat. no. 2983S), anti-cyclin D1 (diluted at 1:1000, CST, cat. no. 55506S), anti-*EFNA1* (diluted at 1:1000, Abcam, cat. no. ab124911), anti-EPHA2 (diluted at 1:1000, Abcam, cat. no. ab273118), anti-LC3 (diluted at 1:1000, CST, cat. no. 12741 T), anti-mTOR (diluted at 1:1000, CST, cat. no. 2983S), anti-p-mTOR (diluted at 1:1000, CST, cat. no. 5536S), anti-p62 (diluted at 1:1000, CST, cat. no. 39749S), anti-p70S6k (diluted at 1:1000, CST, cat. no. 97596S), anti-Rb (diluted at 1:1000, CST, cat. no. 9309S), and anti-p-Rb (diluted at 1:1000, CST, cat. no. 8516S). Expression level of each protein was examined three times.

## 2.6 Cell proliferation and migration assays

KYSE30 and KYSE450 cells with or without *EFNA1* downregulation were seeded into plates or dishes at an appropriate density. Cell proliferation was assessed by Cell Counting Kit-8 (CCK-8) and colony formation assay at indicated time according to previously described [19]. Cell migration was evaluated by wound healing assay as described elsewhere except that cells were cultured in a FBS-free medium for 24 h and then imaged [21].

## 2.7 Cell cycle analysis

KYSE30 and KYSE450 cells were seeded into a 6-well plate at a density of  $3 \times 10^5$  cells/well and cultured at 37 °C with 5% CO<sub>2</sub> for 2 days. After harvested by trypsinization, they were fixed with 70% ethanol at 4 °C overnight. Cells were subsequently washed by precooled PBS and incubated with 100  $\mu$ g/ml RNase A and 50  $\mu$ g/ml propidium iodid (PI) staining solution for 30 min at 4 °C. Then they were immediately analyzed by flow cytometry.

## 2.8 Transmission electron microscopy

ESCC cells were collected and centrifuged at 600 g for 5 min. The pellet was washed and stored in 70% Karnovsky's fixative at 4 °C. Samples were processed and embedded under standard protocols. The ultrathin sections were viewed and photographed using a Hitachi 7000 transmission electron microscope (Tokyo, Japan).

## 2.9 Molecular docking

The three-dimensional structures of 1900 candidate molecules from the MedChemExpress FDA-Approved Drug Library Plus were output using the LigPrep Module of Schrodinger software. We screened for the candidate molecules that potentially bind to EFNA1 by Maestro interface (version 11.4) of Schrodinger software and drew the three-dimensional interaction diagram using PyMol. Top 50 molecules were selected and 45 of them were purchased from MedChemExpress (NJ, USA).

## 2.10 Animal treatment

The female BALB/c nude mice with 6 weeks of age and 18–22 g weight were obtained from the Guangdong Medical Laboratory Animal Center (Guangdong, China). All mice were housed at  $20 \pm 2^\circ\text{C}$  and  $55 \pm 5\%$  relative humidity, with ad libitum access to commercially available food and water throughout the experiment.

KYSE450 cells with or without *EFNA1* knockdown were injected subcutaneously into mice with the concentration of  $1 \times 10^7$  cells/mice, respectively. After 21 days, mice were sacrificed and sampled. The tumors were then measured and weighed to evaluate tumor growth.

The tumor xenografts mice constructed with KYSE450 cells were randomly assigned to four groups as NC, SAA, 5GY and SAA + 5GY. Mice from each group received 100  $\mu\text{l}$  PBS/day orally, 100  $\mu\text{l}$  SAA (20 mg/kg/day) orally, 100  $\mu\text{l}$  PBS/day orally plus 5GY radiation in a single session, and 100  $\mu\text{l}$  SAA (20 mg/kg/day) orally plus 5GY radiation in a single session, respectively. After 21 days the animals were sacrificed and sampled. The tumors were then measured and weighed to evaluate tumor growth.

## 2.11 Statistical analysis

All values were presented as means  $\pm$  standard deviation unless indicated otherwise. Data were analyzed by one-way or two-way analysis of variance (ANOVA) and differences between groups were evaluated using the Student-Newman-Keuls multiple comparison test in SPSS version 20.0. Differences were considered statistically significant at  $p < 0.05$ .

# 3 Results

## 3.1 *EFNA1* was highly expressed in ESCA and significantly correlated with tumor progression

To identify genes essential for ESCA progression, we analyzed the DEGs between cancerous and normal esophageal tissues of patients from TCGA-ESCA, GSE23400, GSE29001, GSE33426, GSE38129 and identified 199 overlapped DEGs (Fig. 1a, b, Additional file 6: Table S3). A total of 173 genes were found expressed with consistent trends (Fig. 1c, Additional file 7: Table S4). Kaplan–Meier curves of survival time were constructed and showed that nine of them were significantly associated with OS, including *APOE*, *ASPM*, *BUB1B*, *EFNA1*, *MAGEA6*, *PBK*, *PUS7*, *TFRC* and *TTK* (Fig. 1d, Additional file 1: Fig. S1a). Receiver operating characteristic (ROC) analysis was further performed and showed that *EFNA1* had the largest area under the curve (AUC) value, indicating the strongest capability in predicting survival rate of ESCA patients (Fig. 1e and Additional file 1: Fig. S1b).

The clinical relevance of other ephrins to ESCA progression was further analyzed due to the abundant evidence that aberrant expression of ephrins was detected in a variety of tumors [22–24]. *EFNA5*, *EFNB1* and *EFNB2* were found highly expressed in tumor tissues of ESCA (Additional file 2: Fig. S2). Yet none of them was significantly correlated with the OS time of ESCA (Additional file 3: Fig. S3a). In addition, the clinical relevance of other ephrins was further validated by ROC analysis, presenting weak capability in predicting survival rate of ESCA patients (Additional file 3: Fig. S3b). Taken together, we found that only *EFNA1* from ephrin ligand family was significantly and positively related to ESCA progression.

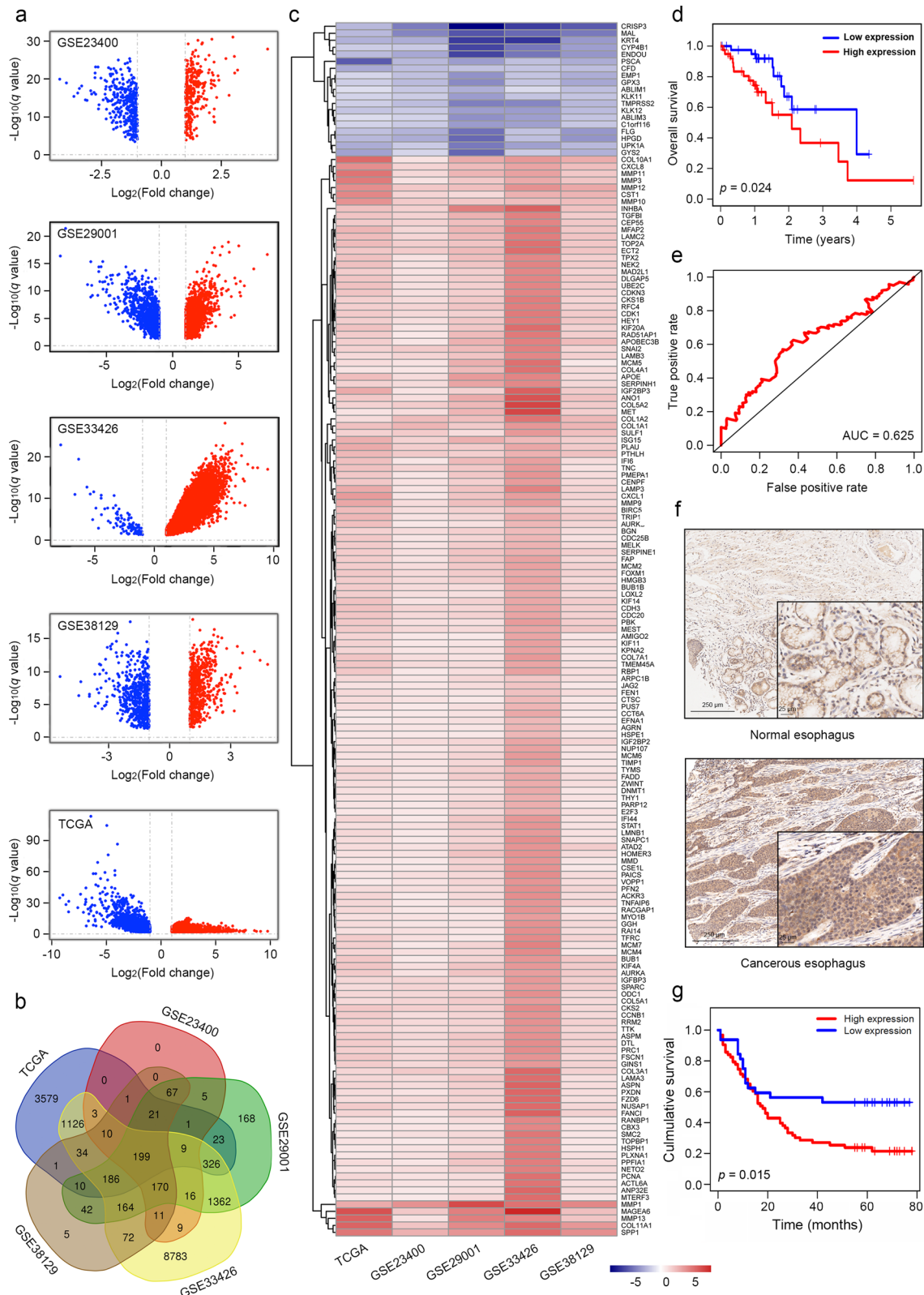


**Fig. 1** *EFNA1* was identified to be essential for ESCA progression. **a** Volcano plot showed the DEGs between ESCA and normal esophageal tissues from public datasets. Red and blue spots represented the upregulated and downregulated genes, respectively. **b** Venn plot showed 199 overlapped DEGs obtained from different dataset. **c** Heatmap showed 173 DEGs with consistent expression trends. **d** Kaplan–Meier curves showed the survival time of ESCA patients with different expression levels of *EFNA1*. **e** ROC analysis showed the capability of *EFNA1* in predicting survival rate of ESCA patients in 3 years. **f** Immunostaining of *EFNA1* in ESCC tissue microarray. **g** Kaplan–Meier curves showed the survival time of ESCA patients with different expression levels of *EFNA1* in tissue microarray

**Table 1** Differential expression of *EFNA1* in normal and cancerous esophagus

|                     | Num | EFNA1 expression |         | Chi-square value | <i>p</i> value |
|---------------------|-----|------------------|---------|------------------|----------------|
|                     |     | High (%)         | Low (%) |                  |                |
| Cancerous esophagus | 63  | 40               | 23      | 4.600            | 0.032*         |
| Normal esophagus    | 63  | 28               | 35      |                  |                |

\*Statistically significant ( $p < 0.05$ )**Table 2** Correlation of *EFNA1* expression to clinical characteristics of ESCC patients

|            | Variables | EFNA1 expression |      | Total | $\chi^2$ | <i>p</i> value |
|------------|-----------|------------------|------|-------|----------|----------------|
|            |           | Low              | High |       |          |                |
| Age (year) | ≤ 65      | 19               | 39   | 58    | 0.004    | 0.951          |
|            | > 65      | 15               | 30   | 45    |          |                |
| Sex        | Female    | 6                | 12   | 18    | 0.001    | 0.974          |
|            | Male      | 28               | 57   | 85    |          |                |
| Grade      | 01-Feb    | 31               | 51   | 82    | 4.182    | 0.041*         |
|            | 03-Apr    | 3                | 18   | 21    |          |                |
| T stage    | T1-T2     | 6                | 18   | 24    | 0.582    | 0.446          |
|            | T3-T4     | 24               | 48   | 72    |          |                |
| N stage    | N0        | 16               | 36   | 52    | 0.238    | 0.625          |
|            | N1-N3     | 18               | 33   | 51    |          |                |
| TNM stage  | 01-Feb    | 15               | 40   | 55    | 0.658    | 0.417          |
|            | 03-Apr    | 15               | 28   | 43    |          |                |

\*Statistically significant ( $p < 0.05$ )

### 3.2 *EFNA1* was essential for cell proliferation and migration in ESCC

Since ESCC is the main subtype of ESCA, the clinical correlations of *EFNA1* to ESCA should be an important reference of those to ESCC. To validate this speculation, we performed immunostaining of *EFNA1* in an ESCC tissue microarray and found that *EFNA1* was highly expressed in cancerous esophagus tissues (Fig. 1f, Table 1). The expression level of *EFNA1* exhibited significantly positive correlation with pathological grading and unfavorable survival (Table 2, Fig. 1g), suggesting a potential role in regulating ESCC progression and prognosis.

To explore the roles of *EFNA1* on tumor progression, we constructed *EFNA1* knockdown cells by transfecting lentivirus containing two independent shRNA targeted to *EFNA1*. qRT-PCR and western blot analysis showed each shRNA could cause remarkably decreased expression of *EFNA1* (Fig. 2a, b). The downregulation of *EFNA1* significantly suppressed the proliferation (Fig. 2c–e) and migration (Fig. 2f, g) of ESCC cells, determined by CCK-8, colony formation and wound healing assays. Furthermore, we constructed xenograft tumors in mice to evaluate the effects of *EFNA1* on tumor growth in vivo. Results showed that knockdown of *EFNA1* significantly suppressed tumor growth on both size and weight (Fig. 2h, i), therefore certifying that *EFNA1* was critical for ESCC proliferation and migration.

### 3.3 *EFNA1* downregulation suppressed cell cycle progression through cMYC in ESCC

To determine the underlying mechanism of *EFNA1* in promoting tumor growth, we analyzed the DEGs between ESCA samples with high and low expression level of *EFNA1* from TCGA dataset. GSEA showed that samples with high expression level of *EFNA1* exhibited significantly aberrant activation of MYC targets, suggesting a positive correlation, which was further confirmed (Fig. 3a, b). The expression level of cMYC was significantly suppressed in *EFNA1*-decreased-cells (Fig. 3c). We further examined the expression levels of several known cMYC target genes in ESCC cells and found that all of them were significantly inhibited when *EFNA1* was downregulated, implying a potentially regulatory role of *EFNA1* on cMYC (Fig. 3d).

Since cMYC is a well-known oncogene tightly correlated with cell cycle progression [25], we examined the expression of several representative cell-cycle-related proteins with *EFNA1* knockdown. Rb, as a cell cycle suppressor, was

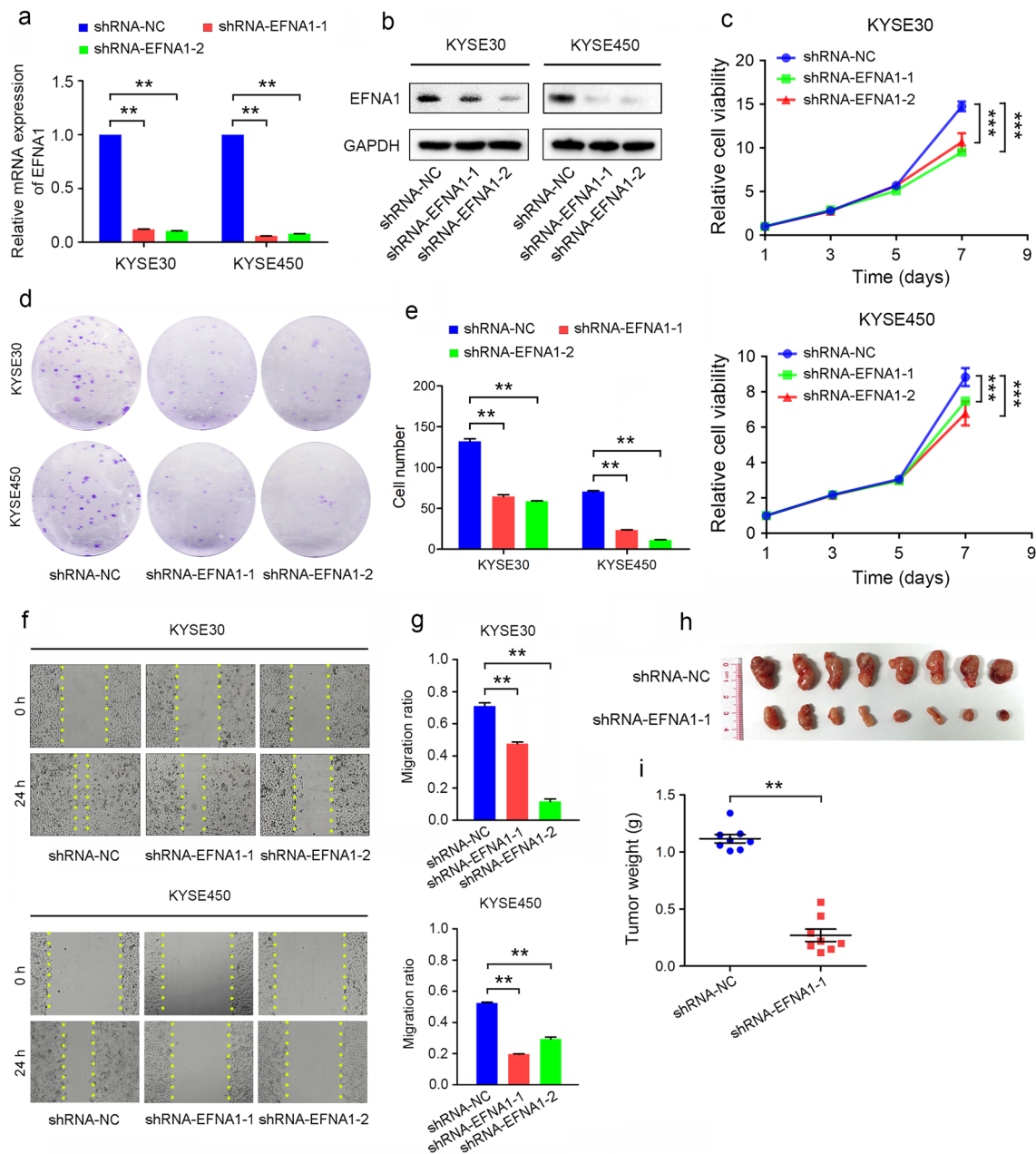


**Fig. 2** Knockdown of *EFNA1* significantly suppressed the proliferation and migration of ESCC cells. **a** qRT-PCR and **b** western blot examined the *EFNA1* knockdown efficiency. **c** CCK-8 and **d** Colony-formation assay showed the cell proliferation with decreased *EFNA1*. **e** Cell counts of the colony-formation assay. **f** Wound healing assay showed the cell migration ability. **g** The migrated distances were measured and analyzed. All values were presented as mean  $\pm$  SD,  $n=3$ , \*  $p < 0.05$ , \*\*  $p < 0.01$ , \*\*\*  $p < 0.001$ , one-way ANOVA was used in **a**, **e** and **g**, two-way ANOVA was used in **c**. **h** The sizes and **i** weights of tumors generated by KYSE30 cells with *EFNA1* knockdown were measured and analyzed. Values were presented as mean  $\pm$  SD,  $n=8$ , \*\*  $p < 0.01$ , one-way ANOVA was used in **i**

barely affected by *EFNA1* downregulation, while the phosphorylated form, which was supposed to promote the transition from G1 to S phase, was significantly suppressed in *EFNA1* knockdown cells (Fig. 3e). Another two critical proteins for cell cycle progression, p-CDC2 and CCND1, were also inhibited by *EFNA1* knockdown (Fig. 3e). Furthermore, we performed flow cytometry analysis to validate that if decreased *EFNA1* could lead to cell cycle arrest and troubled to enter G2/M phase (Fig. 3f, g). Taken together, the *EFNA1*-knockdown-caused inhibition on ESCC growth was approximately through the suppression of cMYC-regulated cell cycle.

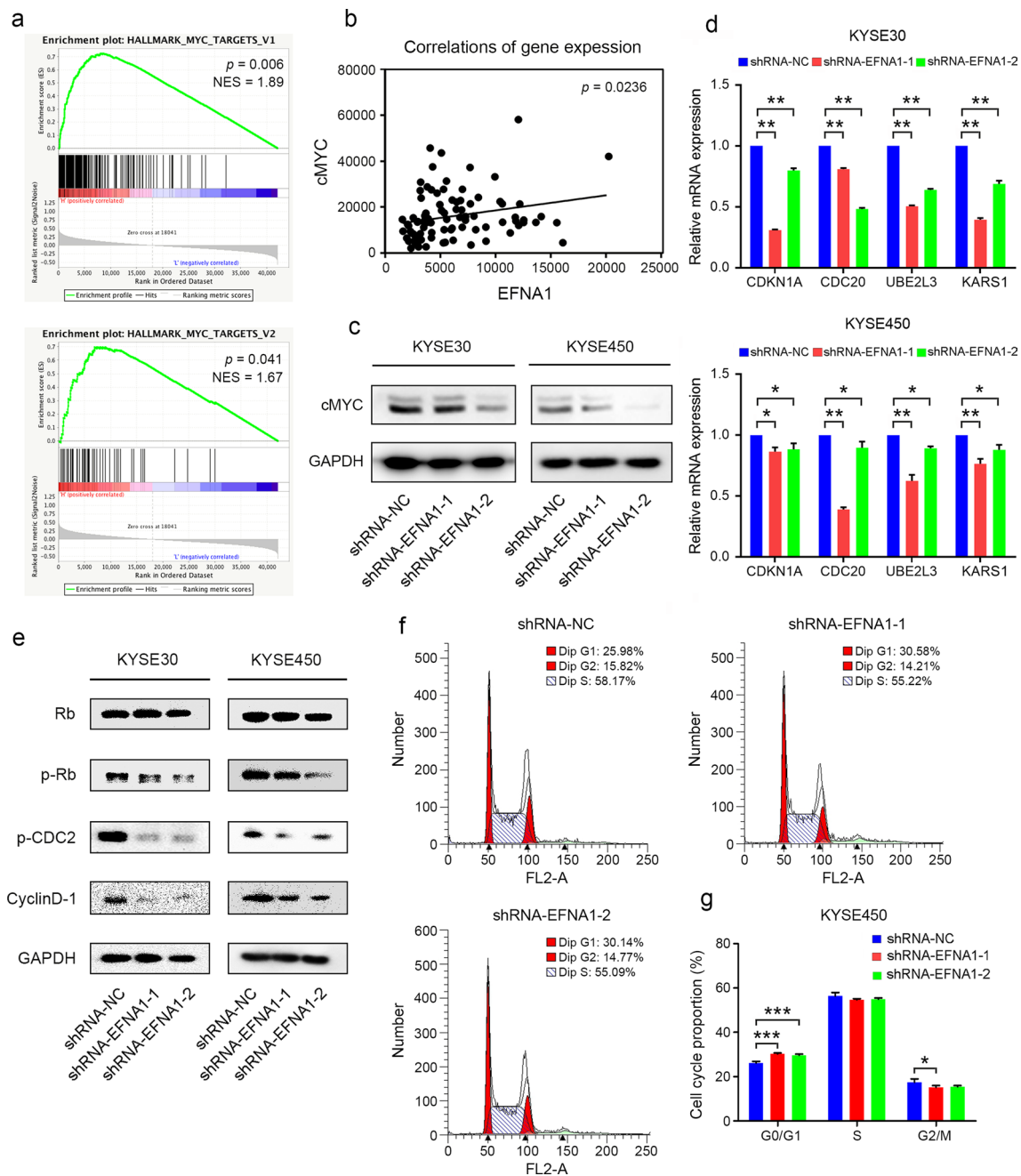


**Fig. 3** Downregulation of *EFNA1* suppressed the expression of *cMYC* and induced cell cycle arrest in ESCC. **a** Representative enrichment plot of DEGs showed that *EFNA1* was significantly associated with *cMYC* targets. **b** Scatter plots showed the expression correlations of *cMYC* and *EFNA1* in ESCA patients from TCGA dataset. **c** Western blot examined the expression level of *cMYC*. **d** qRT-PCR examined the expression levels of the representative *cMYC* target genes **e** Western blot determined the expression levels of cell-cycle-related proteins. **f** and **g** Flow cytometry analysis of cell cycle in ESCC cells with *EFNA1* knockdown. All values were presented as mean  $\pm$  SD,  $n = 3$ , \*  $p < 0.05$ , \*\*  $p < 0.01$ , \*\*\*  $p < 0.001$ , one-way ANOVA was used in **d** and **g**

### 3.4 Knockdown of *EFNA1* activated autophagy in ESCC cells

In addition to the *MYC* targets, ESCA samples with high expression level of *EFNA1* also exhibited significant activation of *mTORC1* signaling, suggesting a potential association with autophagy (Fig. 4a). The autophagy marker *LC3-II* was found upregulated and *p62* was downregulated in *EFNA1* knockdown cells, indicating autophagy activation (Fig. 4b).



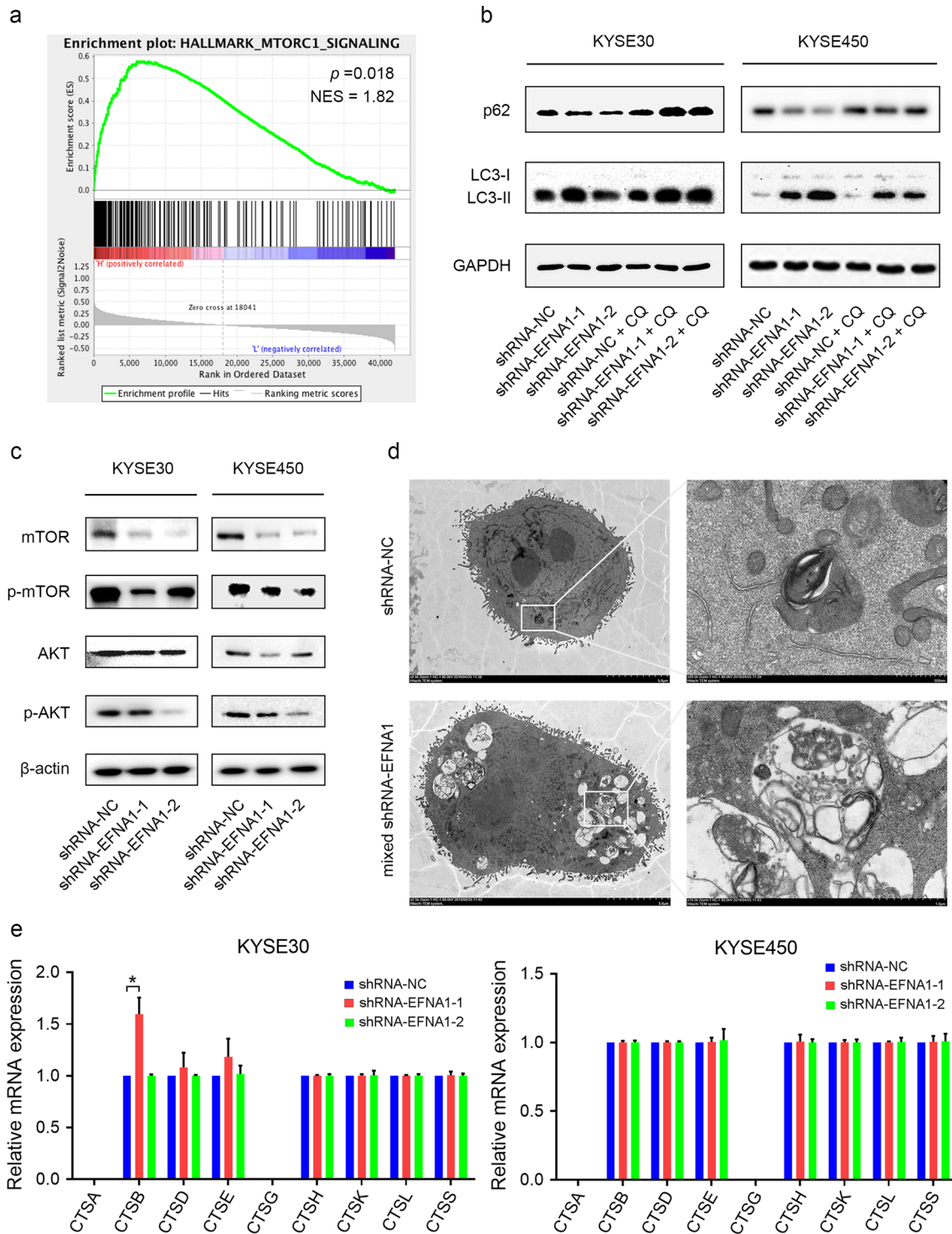


**Fig. 4** Decreased expression of *EFNA1* significantly activated autophagy in ESCC cells. **a** Representative enrichment plot of DEGs showed that *EFNA1* was significantly associated with mTORC1 signaling. **b** Western blot determined the expression levels of autophagy markers, p62 and LC3. **c** Western blot examined the expression levels of representative proteins from Akt/mTOR signaling pathway. **d** Transmission electron microscopy showed the autolysosome in KYSE30 cells with decreased *EFNA1*. **e** qRT-PCR determined the expression levels of cathepsin family members. Values were presented as mean  $\pm$  SD,  $n = 3$ , \*  $p < 0.05$ , one-way ANOVA was used in **e**

**Fig. 5** Knockdown of *EPHA2* showed similar effects on ESCC progression. **a** The potential receptors of EFNA1 predicted with online STRING database. The line thickness indicates the strength of data support. **b** qRT-PCR and **c** Western blot examined the expression level of *EPHA2* in ESCC cells with downregulation of *EFNA1*. **d** qRT-PCR examined the knockdown efficiency of *EPHA2*. **e** CCK-8 assay showed the proliferative capability of ESCC cells with decreased *EPHA2*. **f** and **g** Flow cytometry analysis of cell cycle in KYSE450 cells with *EPHA2* knockdown. All values were presented as mean  $\pm$  SD,  $n=3$ , \*  $p < 0.05$ , \*\*  $p < 0.01$ , \*\*\*  $p < 0.001$ , one-way ANOVA was used in **b** and **d**, two-way ANOVA was used in **e**. **h** Western blot determined the expression levels of autophagy markers and cyclinD-1 in ESCC cells with *EPHA2* knockdown. **i** Schematic illustration showed the potential mechanism of EFNA1 promoting cell proliferation through AKT-regulated cMYC and autophagy in ESCC

To further validate the *EFNA1*-knockdown-induced autophagy activation, we treated the *EFNA1* knockdown cells with the autophagy inhibitor chloroquine (CQ), and examined the expression of LC3-II and p62. The expression levels of these two autophagy markers were significantly increased in *EFNA1* knockdown cells treated with CQ (Fig. 4b). This aberrant accumulation of LC3-II and p62 was approximately caused by CQ-induced sequestration with the persistently activated autophagy caused by knockdown of *EFNA1*.

Since AKT/mTOR was a critical signaling pathway in regulating autophagy, we examined the expression levels of AKT and mTOR along with their corresponding phosphorylated forms and found that all those proteins were downregulated in *EFNA1*-knockdown cells (Fig. 4c). Furthermore, abundant vesiculate structures were detected in *EFNA1*-knockdown ESCC cells by transmission electron microscopy, suggesting autophagolysosome formation and autophagy activation (Fig. 4d). The expression levels of cathepsin family members were further examined to verify that if *EFNA1* downregulation could affect lysosome. Except for *CTSB*, no cathepsin family members exhibited significant differences between normal and *EFNA1* knockdown cells, indicating that *EFNA1* brought no significant effects on lysosome formation (Fig. 4e). Taken together, *EFNA1* knockdown significantly induced autophagy activation, yet whether this suppressed ESCC progression or not remains uncertain and requires further investigation.

### 3.5 Knockdown of *EPHA2* induced similar effects on ESCC progression

EFNA1 is a membrane ligand generally requiring the corresponding receptors to exert its biological functions. The potential receptors matching EFNA1 were explored by online STRING analysis with the experiments proved datasets. A total of 3 receptors binding to EFNA1, including *EPHA2*, *EPHA3* and *EPHA4*, were identified (Fig. 5a). In comparison, *EPHA2* was the most approved receptor and the EFNA1-*EPHA2* interaction was well recognized (Fig. 5a). The expression of *EPHA2* in ESCC cells was validated on both mRNA and protein levels (Fig. 5b, c). Surprisingly, knockdown of *EFNA1* stimulated the expression of *EPHA2* (Fig. 5b, c), which could alleviate the effects of decreased EFNA1 on ESCC cell proliferation and migration on a certain extent.

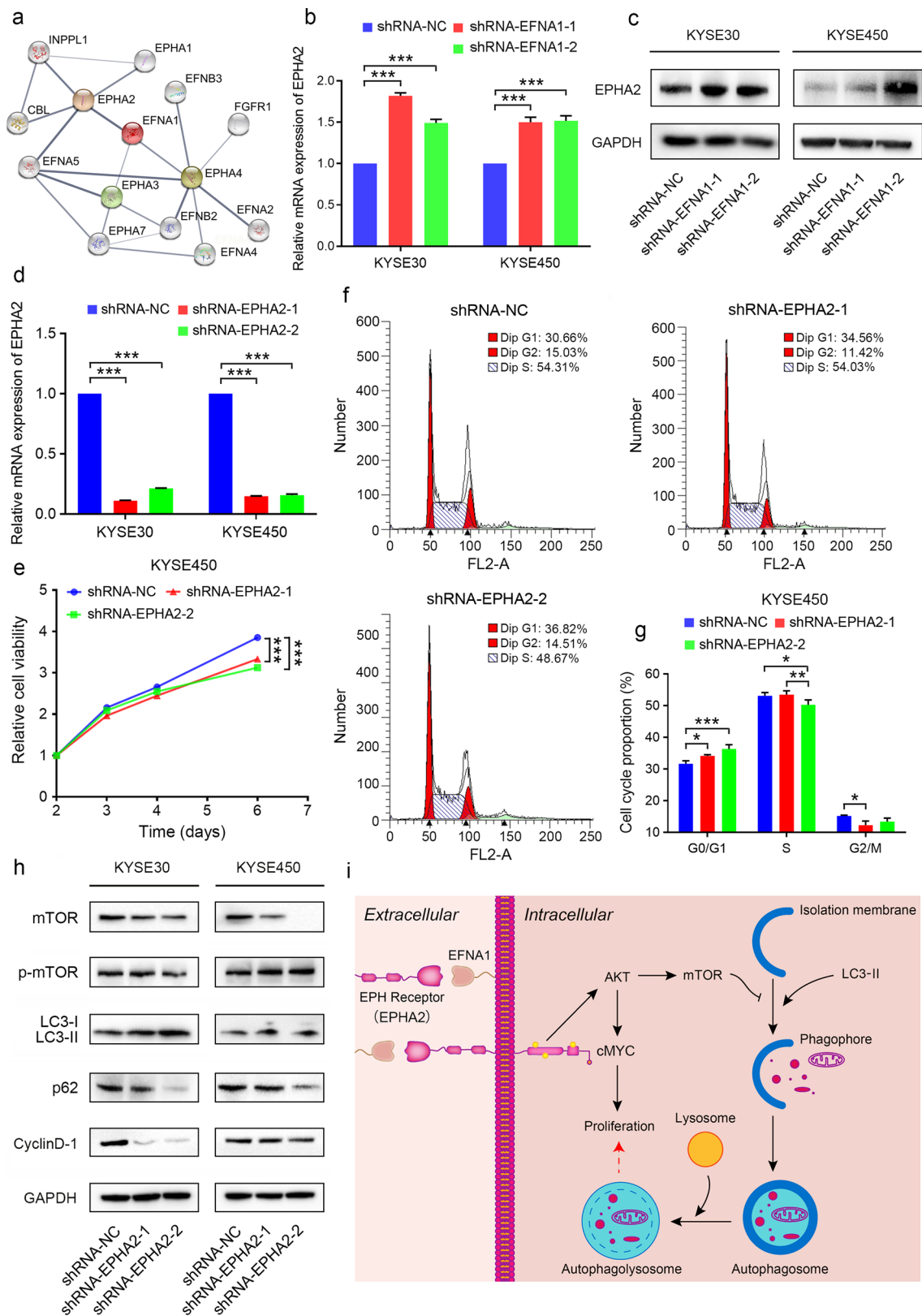
To further validate if *EPHA2* was necessary for EFNA1 promoting ESCC progression, we examined the cell viability of ESCC cells with *EPHA2* knockdown and found that decreased *EPHA2* significantly inhibited cell proliferation (Fig. 5d, e). Flow cytometry analysis showed that *EPHA2* knockdown could also significantly suppress the G1/S transition, similar to the effects caused by *EFNA1* knockdown (Fig. 5f, g). Furthermore, we examined the expression levels of cell cycle marker, cyclinD-1, and several autophagy markers. The expression of cyclinD-1 was significantly suppressed, while the autophagy markers, LC3-II and p62, were upregulated and downregulated, respectively (Fig. 5h). The activation of autophagy was further validated by the suppressed expression of mTOR and the increased expression of p-mTOR (Fig. 5h).

Our findings have described a potential mechanism of EFNA1 promoting ESCC progression. In simple terms, EFNA1 bond to *EPHA2* of the adjacent cells to activate AKT, and thereafter induced the expression of cMYC and mTOR, leading to the persistent proliferation of ESCC cells (Fig. 5i).

### 3.6 SAA was identified as a potential inhibitor targeting EFNA1 for attenuating ESCC progression

Based on the potential therapeutic and prognostic value of *EFNA1*, we performed molecular docking to screen for inhibitors of EFNA1 (Protein Data Bank ID: 3CZU) in the FDA-Approved Drug Library. Drugs binding to the receptor binding domain were selected as candidate molecules targeting to EFNA1 (Fig. 6A, T Additional file 8: Table S5). A total of 45 drugs from the top 50 were purchased and used for evaluating the anti-tumor activities. Most of the drugs exhibited cytotoxic effects on KYSE30 cells, among which salvianolic acid A (SAA) was found to have the most significant anti-tumor activity (Fig. 6b, c).

To validate the inhibitory effects of SAA on ESCC cell proliferation, KYSE30 and KYSE450 cells were treated with various amount of SAA at indicated time. SAA significantly inhibited ESCC cell proliferation in a time and concentration



dependent manner (Fig. 6d, e). We further explored the effects of SAA treatment combined with radiation therapy on ESCC due to the fact that radiotherapy is a clinically critical option to treat ESCC. Each treatment exhibited different levels of inhibition on cell proliferation and in comparison the SAA combined radiation treatment exhibited the

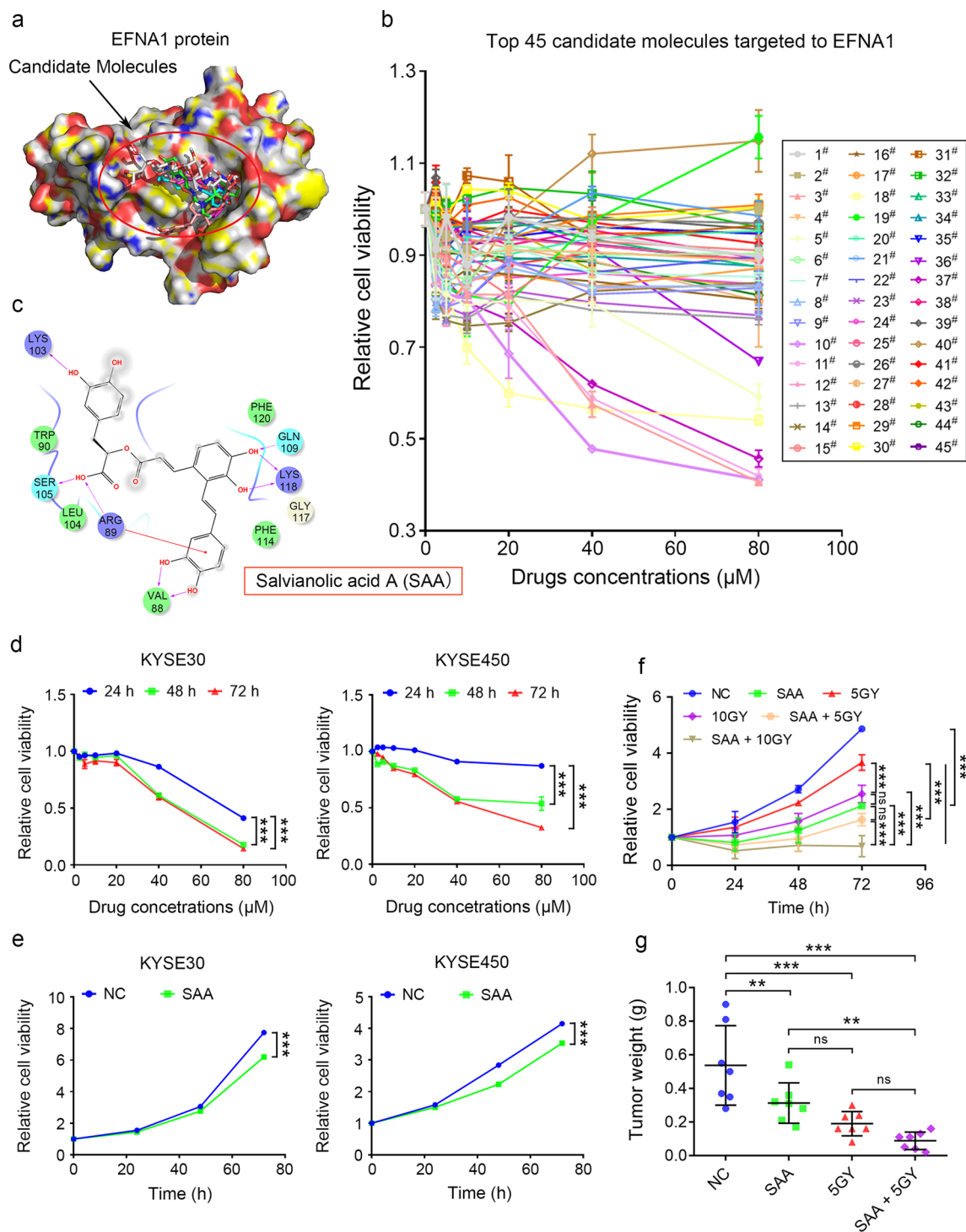


**Fig. 6** SAA was identified as a potential molecule targeting EFNA1. **a** A schematic illustration of EFNA1 binding to small-molecule inhibitors. **b** CCK-8 assay showed the inhibitory effects of 45 from the top 50 molecules on KYSE30 cell proliferation. **c** A two-dimensional model of EFNA1 binding to SAA. **d** CCK-8 assay showed the inhibitory effects of the different concentrations of SAA on ESCC cell proliferation. **e** CCK-8 assay showed the inhibitory effects of 20  $\mu\text{M}$  SAA on ESCC cell proliferation in different time. **f** CCK-8 assay showed the inhibitory effects of 5GY or 10GY radiation with or without the presence of 20  $\mu\text{M}$  SAA. Values were presented as mean  $\pm$  SD,  $n=3$ , ns is short for no significance,  $*** p < 0.001$ , two-way ANOVA was used in **d-f**. **g** The xenograft ESCC tumors from mice treated with SAA and 5GY radiation were weighted. Values were presented as mean  $\pm$  SD,  $n=7$ , ns is short for no significance,  $** p < 0.01$ ,  $*** p < 0.001$ , one-way ANOVA was used in **g**

most severe inhibitory effects (Fig. 6f). The anti-tumor effects of these treatment options on ESCC progression were further validated in mice. Consistently, single SAA or 5GY radiation treatment and the combined treatment all suppressed tumor growth significantly, and the combined treatment showed the most remarkable effects (Fig. 6g). Taken together, these results suggested that SAA significantly suppressed ESCC tumor growth and increase the sensitivity of ESCC to radiotherapy, providing an adjuvant option for treating ESCC in the future.

## 4 Discussion

ESCC is a common malignancy in digestive system characterized by late-stage diagnosis, rapid progression, therapy resistance and poor prognosis [26]. Current treatments for ESCC remain challenging and no targeted therapies have achieved satisfactory outcomes for the patients. In this context, we screened for the critical molecules in ESCC progression with the TCGA and GEO integrated datasets. A total of 9 genes significantly correlated with dismal prognosis were finally identified, including *APOE*, *ASPM*, *BUB1B*, *EFNA1*, *MAGEA6*, *PBK*, *PUS7*, *TFRC* and *TTK*. All these genes have been reported to be significantly associated with tumor progression and poor prognosis in various tumors [27–35]. Here, we performed ROC analysis of these candidate genes and found that in comparison *EFNA1* presented the largest AUC value in predicting survival rate of ESCA patients. Therefore, we further explored the potential roles of *EFNA1* in ESCC progression.

*EFNA1* has been reported to be upregulated in a variety of malignancies and critical for tumor progression. In gastric cancer, high expression level of *EFNA1* was found significantly associated with clinical stage, invasion, lymph node metastasis, recurrence and the rs12904 G > A mutation in 3' UTR increased the susceptibility of the disease [36, 37]. In glioblastoma multiforme, *EFNA1*-*EPHA2* interaction could facilitate the invasion of cancer stem cells via AKT signaling [38]. In bladder cancer, Chu and Zhang showed that *EFNA1* could caused the internalization and downregulation of *EPHA2* on endothelial cells, leading to the activation of angiogenesis [39]. However, there are researches indicating otherwise of *EFNA1* affecting tumor progression. Khodayari et al. showed that *EFNA1* suppressed the malignant mesothelioma via let-7 miRNA inhibiting the expression of RAS [18]. Sukka-Ganesh revealed that *EFNA1* could significantly inhibit cell proliferation and tumor formation in non-small cell lung cancer [15]. Limited studies of *EFNA1* in ESCC showed that high expression of *EFNA1* was found in tumorous tissues and significantly associated with poor prognosis [40]. In this study, we found that downregulation of *EFNA1* could significantly inhibited ESCC cell proliferation, migration and tumor growth in mouse model, suggesting a promoting role of *EFNA1* on ESCC progression.

To explore the underlying mechanism of *EFNA1* facilitating ESCC progression, we analyzed the gene expression profiles of patients with high expression level of *EFNA1*. GSEA showed that high expression of *EFNA1* was positively correlated with cMYC targets and autophagy-related mTORC1 signaling. cMYC, a critical regulator of cell proliferation in tumors [41, 42], was significantly suppressed by decreased *EFNA1*, which was possibly responsible for the cell cycle arrest at G0/G1 phase. Autophagy has been reported to play dual roles in ESCC progression, deficiencies of which could cause the accumulation of oncogenic mutations by DNA damage [43, 44], while the abundance of which promote the survival of tumor cells by relieving the metabolic stress like insufficient nutrient [45, 46]. In this study, we found that decreased *EFNA1* could significantly activate autophagy, while if it was critical for ESCC inhibition was not conclusive. Based our findings, we have learned that the *EFNA1*-promoted ESCC progression could be potentially through the activation of cMYC-mediated cell cycle progression and the inhibition of autophagy.

Due to the currently limited benefits obtained from conventional treatments, more and more attentions have been drawn to targeted therapy on ESCC. Since *EFNA1* was revealed to be essential for ESCC progression in our study, we further explored the potential values of *EFNA1* applied to targeted therapy. Several lines of studies have examined the molecules targeting to *EFNA1* and evaluated the anti-tumor effects. Leflunomide, a common drug for rheumatoid arthritis, has recently been reported to be able to inhibit the angiogenesis and tumor growth in bladder cancer by decreasing the expression of *EFNA1* [39]. Small molecules aiming at the G-H loop of *EFNA1* and the ligand binding domain of *EPHA2*, such as lithocholic acid and the SWL peptide, have also been screened but remained to be tested for tumor treatment [47, 48]. Most of the reported drugs were designed to target the interaction of *EFNA1*-*EPHA2* and overlooked other possibilities, we therefore performed molecular docking to screen for molecules directly binding to *EFNA1* and examined the anti-tumor activity in ESCC. SAA was found to be most effective to suppress ESCC progression, and has been reported capable of inhibiting tumor cell proliferation and invasion in a variety of human malignancies [49–51]. Additionally, SAA could also remarkably increase the sensitivity of ESCC cells to radiation treatment, suggesting a novel therapeutic option for ESCC.

**Acknowledgements** Not applicable.

**Author contributions** HJ, SW and YL performed the experiments. HJ and LC analyzed the RNA-seq data and the clinical correlations of candidate genes. CZ, KZ and ZX analyzed the data obtained from assays. YD and CZ provided the samples. HJ and ZC evaluated the immunohistochemical scores. CZ supervised this project. LF, KL and XM designed the project. XM integrated the data and wrote the manuscript. All authors read and approved the final manuscript.

**Funding** This work was supported by the National Natural Science Foundation of China [82273040], the University Natural Science Research Project of Anhui Province [gzyqZD2021143], and the Basic and Applied Basic Research Foundation of Guangdong Province [2021A151511144].

**Data availability** All data generated from this study are included in this article and the supplementary files.

## Declarations

**Ethics approval and consent to participate** All animal experiments were approved by the Shenzhen People's Hospital Institutional Animal Care and Use Committee (AUP-220302-LKS-085-01), and performed in accordance with the Guidelines for Animal Experimentation of Shenzhen People's Hospital. The tumors in mice used in this study have not exceeded the maximal tumor size approved by the ethics committee.

**Consent for publication** All the authors have significant contributions and in agreement with the content of the manuscript.

**Competing interests** The authors declare that they have no competing interests.

**Open Access** This article is licensed under a Creative Commons Attribution 4.0 International License, which permits use, sharing, adaptation, distribution and reproduction in any medium or format, as long as you give appropriate credit to the original author(s) and the source, provide a link to the Creative Commons licence, and indicate if changes were made. The images or other third party material in this article are included in the article's Creative Commons licence, unless indicated otherwise in a credit line to the material. If material is not included in the article's Creative Commons licence and your intended use is not permitted by statutory regulation or exceeds the permitted use, you will need to obtain permission directly from the copyright holder. To view a copy of this licence, visit <http://creativecommons.org/licenses/by/4.0/>.

## References

1. Sung H, Ferlay J, Siegel RL. Global Cancer Statistics 2020: GLOBOCAN Estimates of Incidence and Mortality Worldwide for 36 Cancers in 185 Countries. *CA Cancer J Clin.* 2021;71(3):209–49. <https://doi.org/10.3322/caac.21660>.
2. Abnet CC, Arnold M, Wei WQ. Epidemiology of Esophageal Squamous Cell Carcinoma. *Gastroenterology.* 2018;154(2):360–73. <https://doi.org/10.1053/j.gastro.2017.08.023>.
3. Hirano H, Kato K. Systemic treatment of advanced esophageal squamous cell carcinoma: chemotherapy, molecular-targeting therapy and immunotherapy. *Jpn J Clin Oncol.* 2019;49(5):412–20. <https://doi.org/10.1093/jjco/hyz034>.
4. Merkow RP, Bilimoria KY, McCarter MD, Chow WB, Ko CY, Bentrem DJ. Use of multimodality neoadjuvant therapy for esophageal cancer in the United States: assessment of 987 hospitals. *Ann Surg Oncol.* 2012;19(2):357–64. <https://doi.org/10.1245/s10434-011-1945-3>.
5. Huang FL, Yu SJ. Esophageal cancer: Risk factors, genetic association, and treatment. *Asian J Surg.* 2018;41(3):210–5. <https://doi.org/10.1016/j.asjsur.2016.10.005>.
6. Chong CR, Jänne PA. The quest to overcome resistance to EGFR-targeted therapies in cancer. *Nat Med.* 2013;19(11):1389–400. <https://doi.org/10.1038/nm.3388>.
7. Gerson JN, Skariah S, Denlinger CS, Astsurov I. Perspectives of HER2-targeting in gastric and esophageal cancer. *Expert Opin Investig Drugs.* 2017;26(5):531–40. <https://doi.org/10.1080/13543784.2017.1315406>.
8. Olsson AK, Dimberg A, Kreuger J, Claesson-Welsh L. VEGF receptor signalling - in control of vascular function. *Nat Rev Mol Cell Biol.* 2006;7(5):359–71. <https://doi.org/10.1038/nrm1911>.
9. Petty RD, Dahle-Smith A, Stevenson DAJ, Osborne A, Massie D, Clark C, Murray GI, Dutton SJ, Roberts C, Chong IY, Mansoor W, Thompson J, Harrison M, Chatterjee A, Falk SJ, Elyan S, Garcia-Alonso A, Fyfe DW, Wadsley J, Chau I, Ferry DR, Miedzybrodzka Z. Gefitinib and EGFR gene copy number aberrations in Esophageal cancer. *J Clin Oncol.* 2017;35(20):2279–87. <https://doi.org/10.1200/jco.2016.70.3934>.
10. Ogitani Y, Aida T, Hagihara K, Yamaguchi J, Ishii C, Harada N, Soma M, Okamoto H, Oitate M, Arakawa S, Hirai T, Atsumi R, Nakada T, Hayakawa I, Abe Y, Agatsuma T. DS-8201a, A Novel HER2-targeting ADC with a Novel DNA topoisomerase I inhibitor, demonstrates a promising antitumor efficacy with differentiation from T-DM1. *Clin Cancer Res.* 2016;22(20):5097–108. <https://doi.org/10.1158/1078-0432.ccr-15-2822>.
11. Spratlin JL, Cohen RB, Eadens M, Gore L, Camidge DR, Diab S, Leong S, O'Bryant C, Chow LQ, Serkova NJ, Meropol NJ, Lewis NL, Chiorean EG, Fox F, Youssoufian H, Rowinsky EK, Eckhardt SG. Phase I pharmacologic and biologic study of ramucirumab (IMC-1121B), a fully human immunoglobulin G1 monoclonal antibody targeting the vascular endothelial growth factor receptor-2. *J Clin Oncol.* 2010;28(5):780–7. <https://doi.org/10.1200/jco.2009.23.7537>.
12. Yang YM, Hong P, Xu WW, He QY. Advances in targeted therapy for esophageal cancer. *Signal Transduct Target Ther.* 2020;5(1):229. <https://doi.org/10.1038/s41392-020-00323-3>.
13. Ieguchi K, Maru Y. Roles of EphA1/A2 and ephrin-A1 in cancer. *Cancer Sci.* 2019;110(3):841–8. <https://doi.org/10.1111/cas.13942>.
14. Shiuian E, Inala A, Wang S, Song W, Youngblood V, Chen J, Brantley-Sieders DM. Host deficiency in ephrin-A1 inhibits breast cancer metastasis. *F1000Res.* 2020. <https://doi.org/10.12688/f1000research.22689.2>.

15. Sukka-Ganesh B, Mohammed KA, Kaye F, Goldberg EP, Nasreen N. Ephrin-A1 inhibits NSCLC tumor growth via induction of Cdx-2 a tumor suppressor gene. *BMC Cancer*. 2012. <https://doi.org/10.1186/1471-2407-12-309>.
16. Iida H, Honda M, Kawai HF, Yamashita T, Shirota Y, Wang BC, Miao H, Kaneko S. Ephrin-A1 expression contributes to the malignant characteristics of  $\alpha$ -fetoprotein producing hepatocellular carcinoma. *Gut*. 2005;54(6):843–51. <https://doi.org/10.1136/gut.2004.049486>.
17. Khodayari N, Mohammed KA, Lee H, Kaye F, Nasreen N. MicroRNA-302b targets Mcl-1 and inhibits cell proliferation and induces apoptosis in malignant pleural mesothelioma cells. *Am J Cancer Res*. 2016;6(9):1996–2009.
18. Khodayari N, Mohammed KA, Goldberg EP, Nasreen N. EphrinA1 inhibits malignant mesothelioma tumor growth via let-7 microRNA-mediated repression of the RAS oncogene. *Cancer Gene Ther*. 2011;18(11):806–16. <https://doi.org/10.1038/cgt.2011.50>.
19. Liu D, Li W, Zhong F, Yin J, Zhou W, Li S, Sun X, Xu J, Li G, Wen Y, Wang J, Hong M, Cheng Z, Yuan J, Dai L, Sun J, Wang J, Qiu C, Wang G, Zou C. METTL7B is required for cancer cell proliferation and tumorigenesis in non-small cell lung cancer. *Front Pharmacol*. 2020. <https://doi.org/10.3389/fphar.2020.00178>.
20. Ma X, Zhang Y, Jiang D, Yang Y. Protective effects of functional amino acids on apoptosis, inflammatory response, and pulmonary fibrosis in lipopolysaccharide-challenged mice. *J Agric Food Chem*. 2019;67(17):4915–22. <https://doi.org/10.1021/acs.jafc.9b00942>.
21. Liu Z, Wang Y, Dou C, Xu M, Sun L, Wang L, Yao B, Li Q, Yang W, Tu K, Liu Q. Hypoxia-induced up-regulation of VASP promotes invasiveness and metastasis of hepatocellular carcinoma. *Theranostics*. 2018;8(17):4649–63. <https://doi.org/10.7155/thno.26789>.
22. Zhao Y, Cai C, Zhang M, Shi L, Wang J, Zhang H, Ma P, Li S. Ephrin-A2 promotes prostate cancer metastasis by enhancing angiogenesis and promoting EMT. *J Cancer Res Clin Oncol*. 2021;147(7):2013–23. <https://doi.org/10.1007/s00432-021-03618-2>.
23. Li Y, Liu DX, Li MY, Qin XX, Fang WG, Zhao WD, Chen YH. Ephrin-A3 and ephrin-A4 contribute to microglia-induced angiogenesis in brain endothelial cells. *Anat Rec (Hoboken)*. 2014;297(10):1908–18. <https://doi.org/10.1002/ar.22998>.
24. Bhatia S, Oweida A, Lennon S, Darragh LB, Milner D, Phan AV, Mueller AC, Van Court B, Raben D, Serkova NJ, Wang XJ, Jimeno A, Clambey ET. Inhibition of EphB4-Ephrin-B2 signaling reprograms the tumor immune microenvironment in head and neck cancers. *Cancer Res*. 2019;79(10):2722–35. <https://doi.org/10.1158/0008-5472.can-18-3257>.
25. Bretones G, Delgado MD, León J. Myc and cell cycle control. *Biochim Biophys Acta*. 2015;1849(5):506–16. <https://doi.org/10.1016/j.bbagem.2014.03.013>.
26. Reichenbach ZW, Murray MG, Saxena R, Farkas D, Karassik EG, Klochkova A, Patel K, Tice C, Hall TM, Gang J, Parkman HP, Ward SJ, Tétreault MP, Whelan KA. Clinical and translational advances in esophageal squamous cell carcinoma. *Adv Cancer Res*. 2019. <https://doi.org/10.1016/bs.acr.2019.05.004>.
27. Zhang Y, Zheng L. Apolipoprotein: prospective biomarkers in digestive tract cancer. *Transl Cancer Res*. 2020;9(5):3712–20. <https://doi.org/10.21037/tcr-19-2106>.
28. Feng Z, Zhang J, Zheng Y, Liu J, Duan T, Tian T. Overexpression of abnormal spindle-like microcephaly-associated (ASPM) increases tumor aggressiveness and predicts poor outcome in patients with lung adenocarcinoma. *Transl Cancer Res*. 2021;10(2):983–97. <https://doi.org/10.21037/tcr-20-2570>.
29. Jiao CY, Feng QC, Li CX, Wang D, Han S, Zhang YD, Jiang WJ, Chang J, Wang X, Li XC. BUB1B promotes extrahepatic cholangiocarcinoma progression via JNK/c-Jun pathways. *Cell Death Dis*. 2021;12(1):63. <https://doi.org/10.1038/s41419-020-03234-x>.
30. Endo M, Kanda M, Sawaki K, Shimizu D, Tanaka C, Kobayashi D, Hattori N, Hayashi M, Yamada S, Koike M, Omae K, Kodera Y. Tissue expression of melanoma-associated antigen A6 and clinical characteristics of gastric cancer. *Anticancer Res*. 2019;39(11):5903–10. <https://doi.org/10.21873/anticancer.13794>.
31. Yu WN, Lin HF, Lee YI, Shia WC, Sung WW, Yeh CM, Lin YM. PBK expression is associated with prognosis of patients with oral squamous cell carcinoma treated with radiotherapy: a retrospective study. *Anticancer Res*. 2021;41(4):2177–82. <https://doi.org/10.21873/anticancer.14991>.
32. Ohashi T, Komatsu S, Ichikawa D, Miyamae M, Okajima W, Imamura T, Kiuchi J, Nishibeppu K, Kosuga T, Konishi H, Shiozaki A, Fujiwara H, Okamoto K, Tsuda H, Otsuji E. Overexpression of PBK/TPK contributes to tumor development and poor outcome of esophageal squamous cell carcinoma. *Anticancer Res*. 2016;36(12):6457–66. <https://doi.org/10.21873/anticancer.11244>.
33. Song D, Guo M, Xu S, Song X, Bai B, Li Z, Chen J, An Y, Nie Y, Wu K, Wang S, Zhao Q. HSP90-dependent PUS7 overexpression facilitates the metastasis of colorectal cancer cells by regulating LASP1 abundance. *J Exp Clin Cancer Res*. 2021;40(1):170. <https://doi.org/10.1186/s13046-021-01951-5>.
34. Huang Y, Huang J, Huang Y, Gan L, Long L, Pu A, Xie R. TFRC promotes epithelial ovarian cancer cell proliferation and metastasis via up-regulation of AXIN2 expression. *Am J Cancer Res*. 2020;10(1):131–47.
35. Liu Y, Zhu K, Guan X, Xie S, Wang Y, Tong Y, Guo L, Zheng H, Lu R. TTK is a potential therapeutic target for cisplatin-resistant ovarian cancer. *J Ovarian Res*. 2021;14(1):128. <https://doi.org/10.1186/s13048-021-00884-z>.
36. Nakamura R, Kataoka H, Sato N, Kanamori M, Ihara M, Igarashi H, Ravshanov S, Wang YJ, Li ZY, Shimamura T, Kobayashi T, Konno H, Shimamura K, Tanaka M, Sugimura H. EPHA2/EFNA1 expression in human gastric cancer. *Cancer Sci*. 2005;96(1):42–7. <https://doi.org/10.1111/j.1349-7006.2005.00007.x>.
37. Li Y, Nie Y, Cao J, Tu S, Lin Y, Du Y, Li Y. G-A variant in miR-200c binding site of EFNA1 alters susceptibility to gastric cancer. *Mol Carcinog*. 2014;53(3):219–29. <https://doi.org/10.1002/mc.21966>.
38. Miao H, Gale NW, Guo H, Qian J, Petty A, Kaspar J, Murphy AJ, Valenzuela DM, Yancopoulos G, Hambardzumyan D, Lathia JD, Rich JN, Lee J, Wang B. EphA2 promotes infiltrative invasion of glioma stem cells in vivo through cross-talk with Akt and regulates stem cell properties. *Oncogene*. 2015;34(5):558–67. <https://doi.org/10.1038/onc.2013.590>.
39. Chu M, Zhang C. Inhibition of angiogenesis by leflunomide via targeting the soluble ephrin-A1/EphA2 system in bladder cancer. *Sci Rep*. 2018;8(1):1539. <https://doi.org/10.1038/s41598-018-19788-y>.
40. Chen FF, Zhang SR, Peng H, Chen YZ, Cui XB. Integrative genomics analysis of hub genes and their relationship with prognosis and signaling pathways in esophageal squamous cell carcinoma. *Mol Med Rep*. 2019;20(4):3649–60. <https://doi.org/10.3892/mmr.2019.10608>.
41. Wang H, Mannava S, Grachtchouk V, Zhuang D, Soengas MS, Gudkov AV, Prochownik EV, Nikiforov MA. c-Myc depletion inhibits proliferation of human tumor cells at various stages of the cell cycle. *Oncogene*. 2008;27(13):1905–15. <https://doi.org/10.1038/sj.onc.1210823>.
42. Cappellen D, Schlange T, Bauer M, Maurer F, Hynes NE. Novel c-MYC target genes mediate differential effects on cell proliferation and migration. *EMBO Rep*. 2007;8(1):70–6. <https://doi.org/10.1038/sj.embor.7400849>.

43. Karantza-Wadsworth V, Patel S, Kravchuk O, Chen G, Mathew R, Jin S, White E. Autophagy mitigates metabolic stress and genome damage in mammary tumorigenesis. *Genes Dev.* 2007;21(13):1621–35. <https://doi.org/10.1101/gad.1565707>.
44. Wu J, Gao F, Xu T, Deng X, Wang C, Yang X, Hu Z, Long Y, He X, Liang G, Ren D, Dai T. miR-503 suppresses the proliferation and metastasis of esophageal squamous cell carcinoma by triggering autophagy via PKA/mTOR signaling. *Int J Oncol.* 2018;52(5):1427–42. <https://doi.org/10.3892/ijo.2018.4320>.
45. Rabinowitz JD, White E. Autophagy and metabolism. *Science.* 2010;330(6009):1344–8. <https://doi.org/10.1126/science.1193497>.
46. Feng Y, Gao Y, Wang D, Xu Z, Sun W, Ren P. Autophagy Inhibitor (LY294002) and 5-fluorouracil (5-FU) combination-based nanoliposome for enhanced efficacy against esophageal squamous cell carcinoma. *Nanoscale Res Lett.* 2018;13(1):325. <https://doi.org/10.1186/s11671-018-2716-x>.
47. Giorgio C, Hassan Mohamed I, Flammini L, Barocelli E, Incerti M, Lodola A, Tognolini M. Lithocholic acid is an Eph-ephrin ligand interfering with Eph-kinase activation. *PLoS ONE.* 2011;6(3):18128. <https://doi.org/10.1371/journal.pone.0018128>.
48. Duggineni S, Mitra S, Lamberto I, Han X, Xu Y, An J, Pasquale EB, Huang Z. Design and synthesis of potent bivalent peptide agonists targeting the EphA2 Receptor. *ACS Med Chem Lett.* 2013;4(3):344–8. <https://doi.org/10.1021/ml3004523>.
49. Tang XL, Yan L, Zhu L, Jiao DM, Chen J, Chen QY. Salvianolic acid A reverses cisplatin resistance in lung cancer A549 cells by targeting c-met and attenuating Akt/mTOR pathway. *J Pharmacol Sci.* 2017;135(1):1–7. <https://doi.org/10.1016/j.jphs.2017.06.006>.
50. Zheng X, Chen S, Yang Q, Cai J, Zhang W, You H, Xing J, Dong Y. Salvianolic acid A reverses the paclitaxel resistance and inhibits the migration and invasion abilities of human breast cancer cells by inactivating transgelin 2. *Cancer Biol Ther.* 2015;16(9):1407–14. <https://doi.org/10.1080/15384047.2015.1070990>.
51. Chuang CY, Ho YC, Lin CW, Yang WE, Yu YL, Tsai MC, Yang SF, Su SC. Salvianolic acid A suppresses MMP-2 expression and restrains cancer cell invasion through ERK signaling in human nasopharyngeal carcinoma. *J Ethnopharmacol.* 2020. <https://doi.org/10.1016/j.jep.2020.112601>.

**Publisher's Note** Springer Nature remains neutral with regard to jurisdictional claims in published maps and institutional affiliations.